Drug Design, Development and Therapy

Dovepress
Taylor & Francis Group

Open Access Full Text Article

ORIGINAL RESEARCH

Leonurine Attenuates CCl_4-Induced Hepatic Fibrosis in Mice via the Hippo-YAP Pathway

Pengru Wang[1,2,*], Junjie Bai[1,2,*], Mingxin Ye[2], Zhiwei Huang[1,2], Jiatong Chen[1,2], Lei Sun[1,2], Xiaolin Zhong[3], Yang Zheng[4], Tingting Ma[5], Wenguang Fu[1,2], Yichao Du[1,6]

[1]Metabolic Hepatobiliary and Pancreatic Diseases Key Laboratory of Luzhou City, Academician (Expert) Workstation of Sichuan Province, the Affiliated Hospital, Southwest Medical University, Luzhou, 646000, People's Republic of China; [2]Department of General Surgery (Hepatopancreatobiliary Surgery), the Affiliated Hospital, Southwest Medical University, Luzhou, 646000, People's Republic of China; [3]Department of Gastroenterology, The Affiliated Hospital of Southwest Medical University, Luzhou, People's Republic of China; [4]Drug Clinical Trial Institution, The Affiliated Hospital of Southwest Medical University, Luzhou, 646000, People's Republic of China; [5]Clinical Medical Research Center, the Affiliated Hospital of Southwest Medical University, Luzhou, People's Republic of China; [6]Department of Gastroenterology, The First Affiliated Hospital of Xi'an Jiaotong University, Xi'an, People's Republic of China

*These authors contributed equally to this work

Correspondence: Wenguang Fu, Department of General Surgery (Hepatopancreatobiliary Surgery), The Affiliated Hospital of Southwest Medical University, Luzhou, 646000, People's Republic of China, Tel +860830-3165200, Fax +8608302392753, Email fuwg@swmu.edu.cn; Yichao Du, Academician (Expert) Workstation of Sichuan Province, the Affiliated Hospital of Southwest Medical University, Luzhou, People's Republic of China, Tel +860830-3165200, Fax +8608302392753, Email duyc@swmu.edu.cn

Background and Purpose: The repair response to persistent damage in the liver manifests as liver fibrosis. Leonurine (Leo), an herbal remedy from traditional Chinese medicine, exhibits multiple biological activities such as antioxidant and anti-inflammatory effects. Nevertheless, research exploring Leo's influence on liver fibrosis remains absent. This study aims to investigate the effect of Leo on liver fibrosis and clarify the mechanisms at play.

Methods: We employed a mouse model of liver fibrosis induced by carbon tetrachloride (CCl_4) and utilized LX-2 cells to investigate the mechanisms through which Leo exerts its effects.

Results: Mice administered CCl_4 displayed an elevated hepatic index, considerable necrosis as revealed by H&E staining, and significantly heightened serum markers of liver injury (ALT and AST). Conversely, mice treated with Leo showed a marked reduction in liver damage, coupled with diminished levels of inflammatory mediators and less infiltration of hepatic macrophages. Importantly, Leo demonstrated protective effects against CCl_4-induced hepatocyte apoptosis in vivo and promoted apoptosis in hepatic stellate cells in vitro. Staining with Sirius red and Masson confirmed that Leo substantially reduced collagen deposition. Furthermore, Leo treatment led to decreased quantities of α-smooth muscle actin (α-SMA) and collagen type I (COL1A1) in both fibrotic tissues and LX-2 cells. Additionally, the administration of Leo was associated with a significant decrease in YAP protein levels, along with an increase in YAP phosphorylation at Ser 397 via the MST-LATS kinase signaling pathway, facilitating the degradation of YAP.

Conclusion: The findings indicate that Leo may exert a protective effect against liver fibrosis through the inhibition of the Hippo-YAP signaling pathway, underscoring its potential as a therapeutic agent for treating hepatic fibrosis.

Keywords: leonurine, liver fibrosis, hepatic stellate cells, apoptosis, cell cycle, yes-associated protein

Introduction

Liver fibrosis represents a pathological alteration of the liver, resulting from a multitude of aetiological factors. It is characterised by an aberrant proliferation of fibrous connective tissue within the hepatic parenchyma. This process is often triggered by factors such as chronic hepatitis, fatty liver or alcoholic liver injury, leading to a gradual decline in liver function.[1] In view of the fact that liver fibrosis has a significant impact on global health, affecting 1–2%[2] of the population, it is imperative that further advances are made in the development of efficacious clinical therapies.[3,4]

Received: 6 February 2025
Accepted: 15 July 2025
Published: 30 July 2025

One of the pivotal stages in the development of liver fibrosis is the activation of hepatic stellate cells (HSCs). HSCs are a class of cells unique to the liver. In normal physiological states, these cells remain in a quiescent state and are crucial for maintaining liver homeostasis, facilitating lipid storage, regulating immune responses, and coordinating the synthesis of the extracellular matrix (ECM).[5,6] During the progression of liver fibrosis, HSCs activate and promote the release of inflammatory mediators, encourage the proliferation of fibrotic cells, and synthesize ECM. Persistent activation of these cells leads to the gradual substitution of the normal liver structure with a fibrous framework made up of collagen and ECM proteins, ultimately disrupting the liver's normal physiological functions. In severe cases, this condition can advance to cirrhosis, which may subsequently result in liver failure, hypertension, and various associated complications.[7]

The Hippo signaling pathway, together with its downstream effector termed Yes-associated protein (YAP), which primarily regulates cell growth, proliferation and apoptosis. It first discovered in Drosophila, has undergone extensive study in mammals.[8] In this pathway, the Hippo kinase complex inhibits the activity of YAP by phosphorylating it, thereby limiting cellular hyperproliferation and tissue overgrowth. The regulation of this process involves the kinase cascade reaction of MST-LATS. During this process, phosphorylated MST1/2 triggers the phosphorylation of LATS1/2, which then facilitates the phosphorylation of YAP at various serine residues. This ultimately results in either the degradation of YAP or its translocation to the nucleus.[9,10] Recent studies have offered further evidence supporting the idea that lowering YAP activity could have a positive impact on the treatment of liver damage and fibrosis. By reducing YAP's activity, it might be feasible to alleviate the adverse effects linked to liver diseases. These results suggest that YAP could serve as an encouraging target for creating innovative therapeutic approaches focused on liver repair and enhancing overall liver health.[11,12]

Herbs are widely used in contemporary medical practice for the treatment of various diseases. Leonurine (Leo, chemical formula $C_{14}H_{21}N_3O_5$, shown in Figure 1A, B) is an active alkaloid extracted from motherwort (*Leonurus japonicus Houtt)*.. This compound is widely used in traditional Chinese medicine and has received increasing research attention for its remarkable efficacy in the treatment of a variety of diseases,[13–15] especially in the treatment of liver injury and fibrosis. Studies have shown that Leo exerts significant protective effects against liver injury through multiple mechanisms (eg, reduction of oxidative stress, inflammation, and fibrosis markers). For example, Yu et al (2023)[16] found that Leo significantly attenuated acetaminophen-induced acute liver injury in mice, which was achieved through enhanced phosphorylation of PI3K, Akt1, and GSK3β. It has also been suggested that Leo may play a role in the protection of experimental non-alcoholic steatohepatitis (NASH) through the AMPK/SREBP1 signaling pathway.[17] In addition, Leo has demonstrated significant efficacy in the treatment of fibrosis in several organs, including the heart and kidney.[18,19] In a myocardial fibrosis model, Leo significantly reduced Angiotensin II–induced NADPH oxidase 4 (Nox4) activation, reactive oxygen species (ROS) production, matrix metalloproteinase 2/9 (MMP 2/9), and the expression of α-smooth muscle actin (α-SMA) and collagen I and III. In addition, Leo (7.5, 15, and 30 mg/kg/day for 42 days) inhibited myocardial fibrosis in rats after myocardial infarction, which was achieved by down-regulating Nox4 expression, ROS, NF-κB activation, and plasma MMP-2 activity.[20] However, knockdown of miR-29a-3p or use of PFT-α, a p53 inhibitor, completely negated the therapeutic effect of Leo on myocardial fibrosis, as evidenced by increased levels of TGF-β, collagen III, and collagen I proteins in cardiac fibroblasts.[21] In the context of liver fibrosis, Leo exhibits protective effects through multiple mechanisms. However, current data on the application of Leo in liver fibrosis are still relatively limited. The aim of this study was to investigate the role of Leo in liver fibrosis models and to elucidate its potential molecular mechanisms, with a view to providing more scientific evidence for the application of Leo in the treatment of liver fibrosis.

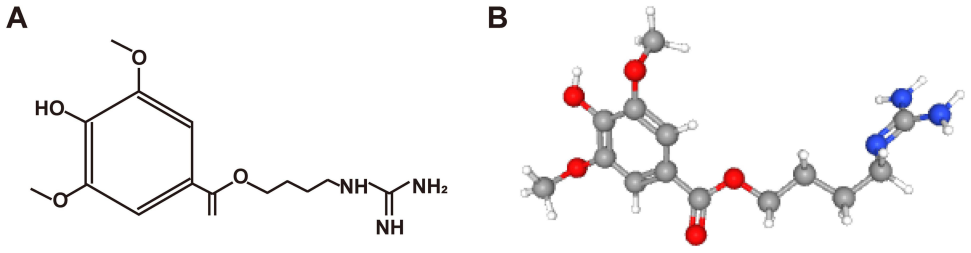

Figure 1 Two-dimensional structure (**A**) and three-dimensional (**B**) structure of Leonurine.

Materials and Methods

Animals

A total of thirty male C57BL/6 mice, each at the age of 8 weeks and weighing around 20 ± 2 g, were procured from Beijing Huafukang Biotechnology Co. The procedures involving these mice were performed in accordance with the protocols sanctioned by the Animal Care and Use Committee at Southwestern Medical University, as indicated by reference number 20221111–003.

Reagents

The reagents and kits used in this study are shown in Table 1.

Animal Model of Hepatic Fibrosis and Experimental Design

A total of thirty mice, raised under normal conditions, were randomly allocated into five distinct groups based on their body weight (n=6/group): (1) control group (Control); (2) the Leo 30 mg/kg group (Leo 30); (3) the CCl_4 group (CCl_4); (4) the CCl_4 + Leo 15 mg/kg group (CCl_4 + Leo 15); (5) the CCl_4 + Leo 30 mg/kg group (CCl_4 + Leo 30). According to the research methods in the previous literature,[2] the control group was administered an intraperitoneal injection of 2.5 mL/kg of olive oil. In the groups treated with CCl_4, CCl_4 + Leo 15, and CCl_4 + Leo 30, a dose of 2.5 mL/kg of CCl_4—diluted at a 1:4 ratio in olive oil—was given via injection two times per week over a period of 8 weeks. During the sixth week, the CCl_4 + Leo 15 and CCl_4 + Leo 30 groups received injections of the respective concentrations of Leo four times weekly for a span of two weeks (Figure 2A).

Table 1 The Reagents and Kits Used in This Study

Product	Company	Cat. No.
Leonurine (purity: 99.64%)	MedChemExpress	HY-N0741
CCl_4 (purity: 98%)	Rhawn Chemical Biochemical Chemical	R019799
Olive oil	MACKLIN	O815210
DMEM	Gibco	C11995500BT
FBS	Gibco	10091148
P/S	Beyotime	C0222
CCK-8	GLPBIO	GK10001
PFA	MACKLIN	P885233
H&E	Solarbio	G1120
Sirius red	Solarbio	G1472
Masson	Solarbio	G1340
DAPI	Beyotime	C1005
ALT	Nanjing Jiancheng	C009-2-1
AST	Nanjing Jiancheng	C010-2-1
LDH	Nanjing Jiancheng	A020-2-2
TNF-α	Yancheng Meimian	MM-0132M1
IL-1β	Yancheng Meimian	MM-0040M1
IL-6	Yancheng Meimian	MM-0163M1
PVDF	Thermo Scientific	88520
TBST	Servicebio	G2150
ECL	Vazyme	E411
RNA extraction	Vazyme	RC113-01
SYBR Green fluorescent	Vazyme	Q341-02
DNase-free proteinase K	Beyotime	ST535
PBS	Servicebio	G4202
TUNEL	Beyotime	C1088

https://doi.org/10.2147/DDDT.S518793

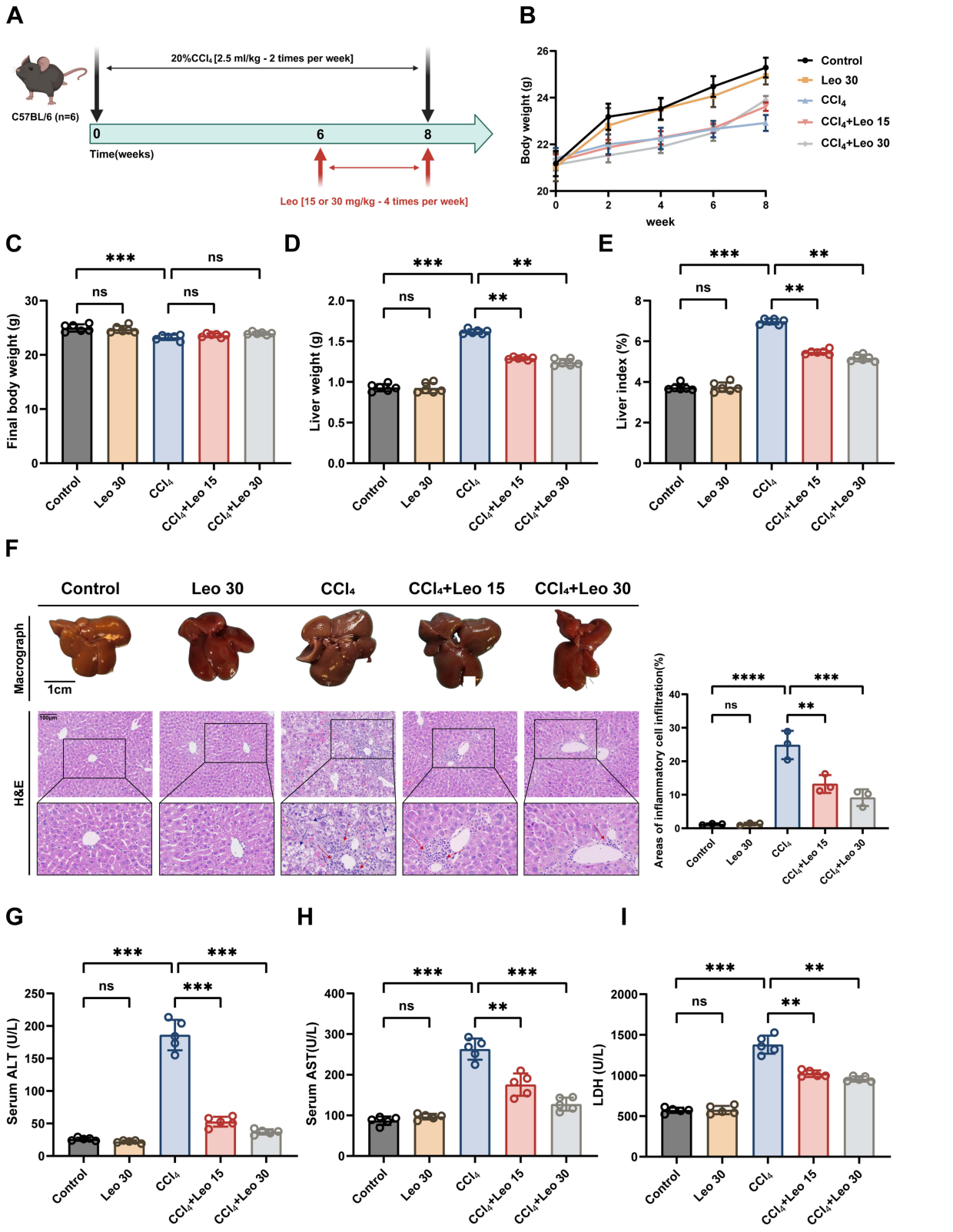

Figure 2 Leonurine effectively alleviated liver injury caused by CCl_4. (**A**) C57BL/6 modeling diagram. (**B**) Body weight change in mice. (**C**) Final body weight (g). (**D**) Liver weight (g). (**E**) Liver index (%). (**F**) Macroscopic (scale bar, 1 cm) and Hematoxylin and Eosin staining images of mouse liver (Red arrows mark inflammatory cells, blue arrows mark vacuolation and necrosis) (scale bar, 100 μm) and quantitative analysis results. (**G-I**) Serum Alanine Aminotransferase (**G**), Aspartate Aminotransferase (**H**), and Liver Lactate Dehydrogenase (**I**) in mice. Data are expressed as mean ± standard deviation. **P<0.01, ***P<0.001, ****P<0.0001.

Abbreviation: ns, no significance.

https://doi.org/10.2147/DDDT.S518793

LX-2 Cell Culture

The LX-2 cell line utilized in this study was procured from Zhongqiaoxinzhou Biotechnology Co., Ltd., located in Shanghai, China. In the laboratory, these cells were cultured using Dulbecco's Modified Eagle Medium (DMEM), which was specifically enhanced by the inclusion of 10% fetal bovine serum (FBS) and a penicillin/streptomycin (P/S) mixture at a dosage of 100 U/mL. The cultures were kept in a controlled environment, a humidified incubator, where the temperature was consistently maintained at 37 °C and supplied with 5% CO_2 to create optimal growth conditions. Prior to the collection of experimental data, the LX-2 cells underwent treatment with varying concentrations of Leo, specifically at 1, 2, and 5 μM, for a duration of 24 h to assess the effects of this compound on cellular behavior.

Cell Counting Kit-8 (CCK-8) Assay

For the assessment of cell viability and proliferation, a suspension of LX-2 cells was carefully seeded into 96-well culture plates at a density of 5×10^3 cells per well. After giving the cells adequate time to adhere to the plate surface, the culture medium was replaced with a serum-free medium containing different concentrations of Leo—1, 2, and 5 μM—to facilitate the experimental treatments. Following a 24-h incubation period, the medium was again replaced, and 10 μL of CCK-8 solution was pipetted into each well. The plates underwent a further incubation at 37 °C for 1 h, allowing the dye to react with the viable cells. The quantitative measurement of the yellow formazan dye produced by the dehydrogenase activity in the living cells was carried out using a Cytation-5 multifunctional microplate reader (BioTek, USA). The absorbance readings obtained from this measurement provided vital information regarding the proliferative activity of the LX-2 cells under the influence of the tested concentrations of Leo.

Histopathological and Immunohistochemistry

Liver samples were maintained in a 4% paraformaldehyde (PFA) solution before being embedded in paraffin. The staining techniques for hematoxylin and eosin (H&E), Sirius red, and Masson's trichrome were performed following the manufacturer's instructions. Immunohistochemistry (IHC) utilized relevant antibodies. Image analysis was conducted using version 1.52 of ImageJ software (Bethesda, MD, USA).

Immunofluorescence Staining

In the process of immunofluorescence staining for LX-2 cells, a total of 7×10^4 cells per well were seeded into 24-well plates. After ensuring cell attachment through microscopic assessment, various concentrations of Leo (1, 2, or 5 μM) were applied for a duration of 24 h. Then, cells were fixed with a 4% paraformaldehyde solution and subsequently permeabilized for antibody staining. The primary antibody against YAP was diluted 1:400 and incubated overnight at 4 °C. Following this step, a secondary antibody was added, and DAPI staining was performed to visualize the nuclei. The cells underwent thorough washing with PBS to eliminate any unbound antibodies, and fluorescence signals were captured using an Olympus fluorescence microscope from Tokyo, Japan.

Biochemical Markers in Serum and Hydroxyproline Levels in Liver Tissues

The evaluation of serum alanine aminotransferase (ALT), aspartate aminotransferase (AST), and lactate dehydrogenase (LDH) levels, along with the hydroxyproline concentration in liver tissues, was executed according to the protocols set by Nanjing Jiancheng Bioengineering Research for assessment.

ELISA Measurement

The serum concentrations of inflammatory markers TNF-α, IL-1β, and IL-6 were quantified following the instructions from Yancheng Meimian Industrial Co., Ltd., China.

Western Blotting

The experiment was conducted in accordance with previously established methods.[22] Table 2 provides a detailed overview of the primary antibodies utilized in this research. To initiate the experiment, equal quantities of protein samples were subjected to electrophoresis on 8–12% SDS-PAGE gels. Following this separation process, the proteins

Table 2 Primary Antibody Used for Western Blot

Antibody	Company	Cat. No.	Dilution
α-SMA	Abcam	ab124964	1:1000
COL1A1	Abcam	ab138492	1:1000
CDK2	Proteintech	10122-1-AP	1:2000
CDK4	Proteintech	11026-1-AP	1:2000
CyclinD1	Proteintech	60186-1-Ig	1:5000
CyclinE1	Proteintech	11554-1-AP	1:2000
PCNA	Proteintech	10205-2-AP	1:5000
Bax	Proteintech	60267-1-Ig	1:5000
Bcl-2	Santa	sc-56018	1:1000
Caspase-3	Proteintech	66470-2-Ig	1:1000
CHOP	Proteintech	15204-1-AP	1:2000
MST1	Proteintech	22245-1-AP	1:1000
MST2	Proteintech	12097-1-AP	1:1000
Phospho-MST1 (Thr183)/MST2 (Thr180)	Proteintech	80093-1-RR	1:2000
LATS1	Proteintech	17049-1-AP	1:1000
Phospho-LATS1/2 (Ser909/Ser872)	Proteintech	28998-1-AP	1:1000
YAP1	Proteintech	66900-1-Ig	1:5000
Phospho-YAP1 (Ser127)	Affinity	AF3328	1:1000
Phospho-YAP1 (Ser397)	Proteintech	29018-1-AP	1:1000
GAPDH	Proteintech	60004-1-Ig	1:2000

were transferred to PVDF membranes to facilitate subsequent analysis. The membranes were then subjected to a blocking step with a 5% skim milk solution at room temperature for a duration of 1 h. This blocking step was crucial to prevent non-specific binding of antibodies during the incubation phase. After the blocking process, the membranes were incubated overnight at 4 °C with diluted primary antibodies to ensure effective binding. Subsequently, the membranes underwent three washing cycles with Tris-buffered saline containing 0.1% Tween 20 (TBST) to remove excess and unbound primary antibodies. A secondary antibody, which was HRP-conjugated and diluted to a concentration of 1:10000 in TBST, was then applied to the membranes and allowed to incubate at room temperature for 1 h. Following the secondary antibody incubation, the membranes were again washed with TBST to eliminate any remaining unbound antibodies. The visualization of protein bands on the membranes was achieved using an ECL kit, and detection was performed with the help of the Vilber Fusion imaging system (Vilber Lourmat, Paris, France). Finally, the gray values of the protein bands were quantified with ImageJ software, version 1.52, developed in Bethesda, MD, USA, allowing for a precise measurement of protein expression levels in the samples analyzed.

Quantitative Real-Time PCR (qRT-PCR) Analysis

Total RNA was extracted from mouse liver tissue as well as LX-2 cells using an RNA extraction kit supplied by Vazyme. Following this extraction, the RNA samples were reverse transcribed following the specific protocol outlined by the reagent vendor, ensuring accurate conversion of RNA to complementary DNA (cDNA). For the qRT-PCR process, the SYBR Green fluorescent reagent, also provided by Vazyme, was utilized, and the amplification reactions were monitored using a QuantStudio 3 detection system from Thermo Fisher Scientific. To ensure reliable and accurate quantification of RNA expression levels, the results were normalized against the expression of the endogenous gene GAPDH, which serves as a reference for comparison. The specific sequences of the PCR primers used in this analysis are detailed in Table 3, allowing for reproducibility and validation of the experimental procedure.

TdT-Mediated dUTP Nick-End Labeling (TUNEL) Assay

Liver tissue paraffin blocks were cut into 4 μm thick sections. A DNase-free proteinase K solution was applied dropwise at a concentration of 20 μg/mL, and the sections were incubated at room temperature for 15 min. After incubation, the

Table 3 Primer Sequence for qRT-PCR Analysis

Species	Gene	Forward Primer	Reverse Primer
Mouse	*TNF-α*	CATCTTCTCAAAATTCGAGTGACAA	TGGGAGTAGACAAGGTACAACCC
	IL-6	ATGGATGCTACCAAACTGGAT	TGAAGGACTCTGGCTTTGTCT
	IL-1β	CGCAGCAGCACATCAACAAGAG	TGTCCTCATCCTGGAAGGTCCACG
	α-SMA	CCCAGACATCAGGGAGTAATGG	TCTATCGGATACTTCAGCGTCA
	COL1A1	TGACTGGAAGAGCGGAGAGT	GTTCGGGCTGATGTACCAGT
	ANKRD1	TTCGAGGCACAAGGCACAA	CCATCATTTCACTGGCGAGC
	CTGF	AAGAGAGGGCCCACGTGTA	GAAGGAGCTGTCTGTTCCACA
	GAPDH	AGCTTCGGCACATATTTCATCTG	CGTTCACTCCCATGACAAACA
Human	*α-SMA*	CCTTGTTTGGGAAGCAAGTGG	TGGAGCTGCTTCACAGGATT
	COL1A1	GTGCGATGACGTGATCTGTGA	CGGTGGTTTCTTGGTCGGT
	YAP1	AGCCCAAGAACAGAAAGAACCT	TTGGACAAGTCCAGTGAGGC
	GAPDH	GACCTGCCGTCTAGAAAAAC	TTGAAGTCAGAGGAGACCAC

sections were washed three times with phosphate-buffered saline to remove excess enzyme. The TUNEL assay was then conducted using a reaction mixture for 1 hour at room temperature. After the TUNEL reaction, nuclei were stained with DAPI. TUNEL-positive cells were examined with fluorescence microscopy (Olympus, Tokyo, Japan) and quantified using ImageJ software, version 1.52 (Bethesda, MD, USA).

Statistical Analysis

The findings of the study are expressed as mean values ± standard deviations (SD). Before conducting statistical analyses using GraphPad Prism version 10.1.2 (California, USA), we performed normality tests (Shapiro–Wilk test) to verify the data distribution. A one-way ANOVA was used to compare group means, followed by Tukey's HSD post-hoc test for pairwise comparisons. P-values < 0.05 were considered statistically significant.

Results

Leo Ameliorates CCl_4-Induced Liver Injury in Mice

During the first six weeks, weight gain among all mice treated with CCl_4 was significantly slower compared to those in the control group. However, after Leo was administered at week six, the mice's weight increased relative to the group receiving CCl_4 (Figure 2B). Following this, the liver index was calculated based on both the final body weights and liver weights of the mice, serving as an indicator of liver injury severity. Mice treated with CCl_4 alone showed a pronounced increase in their liver index compared to the control group. In contrast, a significant reduction in the liver index was noted post-Leo treatment when compared to the CCl_4 group. These results imply that liver injury was mitigated in the mice (Figure 2C–E). The liver coloration of the CCl_4 group was darker than that of the control group, and the liver surface appeared less smooth. After Leo treatment, these conditions improved, with HE staining revealing this alteration more clearly. Notably, many hepatocytes in the CCl_4 group appeared swollen and necrotic, accompanied by considerable infiltration of inflammatory cells in the liver tissue, which saw significant alleviation following Leo treatment (Figure 2F). Biochemical liver function indices, including ALT, AST, and LDH, were evaluated next. The study results showed that serum levels of ALT, AST, and LDH were significantly higher in the CCl_4 group compared to the control group, indicating liver injury. Treatment with Leo significantly reduced these enzyme levels, demonstrating its protective effects on the liver (Figure 2G–I). Additionally, there were no significant differences in these markers between the Leo-treated and control groups, suggesting that Leo was given at a safe dosage. Overall, the findings indicate that Leo effectively protects against liver damage induced by CCl_4.

Leo Reduced CCl_4-Induced Inflammatory Cytokines Expression in vivo

Previous research has indicated that Leo is effective in reducing inflammatory processes and that it inhibits the hepatic inflammatory factor expression induced by acetaminophen.[16] In liver fibrosis, persistent inflammation significantly contributes to fibrosis progression and scar tissue formation. Our study aimed to investigate the anti-inflammatory effects of Leo in the context of CCl_4-induced liver fibrosis. We measured inflammatory factor levels in serum using ELISA and in tissue samples via qRT-PCR. Results showed consistent findings across both methods: the CCl_4 group exhibited significantly elevated levels of TNF-α, IL-6, and IL-1β compared to the control group. In contrast, the Leo-treated group displayed significantly reduced expression of these inflammatory markers compared to the CCl_4 group (Figure 3A–F). Additionally, IHC analysis revealed that the infiltration of CD68 and F4/80 macrophages was substantially lower in the CCl_4 + Leo group compared to the CCl_4 group (Figure 3G). Overall, these findings suggest that Leo has the potential to alleviate inflammation induced by CCl_4 in liver fibrosis.

Leo Mitigates Liver Fibrosis Induced by CCl_4 in Mice

Masson and Sirius red staining techniques were utilized to assess the degree of hepatic fibrosis, aiming to explore the possible role of Leo in this context. The administration of CCl_4 led to the buildup of collagen fibers within the hepatic tissue of the mice. In contrast, treatment with Leo resulted in a significant decrease in this buildup (Figure 4A and B). Additionally, the content of HYP in the liver tissues was significantly higher in the CCl_4 group compared to the control group. Nevertheless, after Leo treatment, this rise was reduced to varying extents (Figure 4C). These results indicate that Leo has the potential to mitigate the advancement of hepatic fibrosis.

Leo Inhibiting Activation of HSCs in vivo

As illustrated in Figure 5A, the mRNA expression levels of *COL1A1* and *α-SMA* were significantly elevated in the liver of the CCl_4 treatment group. Conversely, the group treated with both CCl_4 and Leo showed reduced mRNA levels of *COL1A1* and *α-SMA*. Subsequently, Western blot analysis was conducted to assess protein levels of α-SMA, a marker for the activation of hepatic stellate cells, as well as extracellular matrix proteins COL1A1 and MMP2. The results indicated that liver tissues from mice treated with CCl_4 had higher levels of α-SMA, COL1A1, and MMP2 compared to the control group. Additionally, Leo treatment resulted in a significant reduction in these fibrosis markers in comparison to the CCl_4 group (Figure 5B). This finding was further confirmed by α-SMA IHC staining (Figure 5C), suggesting that Leo effectively inhibits HSC activation induced by CCl_4 in vivo.

Leo Inhibits HSCs Proliferation and Activation in vitro

Studies have shown that the cell cycle of HSCs plays a vital role in the progression of liver fibrosis. When there is liver damage and inflammation, these cells are stimulated by particular signals that encourage them to become activated and transition into a state marked by increased activity. This activation is pivotal as it initiates their involvement in the processes of cell proliferation and the formation of fibrous tissue. As a result of these processes, the cell cycle of hepatic stellate cells experiences significant changes, leading to an increase in the rate of cell division and proliferation. This surge in activity ultimately contributes to the excessive production of fibrous tissue, which is a hallmark of liver fibrosis.[23] In this research, a 24-h self-activation procedure was conducted on LX-2 cells before they received Leo treatment, which ensured the activation of HSCs.[24,25] Our initial experiments investigated how Leo affects LX-2 cell proliferation using the CCK-8 assay. The results showed that Leo significantly inhibits cell proliferation in a dose-dependent manner, with concentrations of 2.5 and 5 μM being particularly effective. The highest concentration of 5 μM demonstrated the most pronounced inhibitory effect, as shown in Figure 6A. To further explore this effect, we treated LX-2 cells with varying concentrations of Leo (1, 2, and 5 μM) for 24, 48, and 72 h. The CCK-8 assay results indicated that a 24-h pre-treatment with Leo was most effective in suppressing cell proliferation, significantly reducing LX-2 cell growth (Figure 6B). Consequently, we conducted subsequent experiments using LX-2 cells pre-treated with Leo at concentrations of 1, 2, and 5 μM for 24 h. In order to evaluate the expression levels of proteins associated with the cell cycle, Western blot analysis was performed. The results of this analysis demonstrated that treatment with 5 μM Leo led to a significant reduction in the expression of several key proteins, specifically CDK4, CyclinD1,

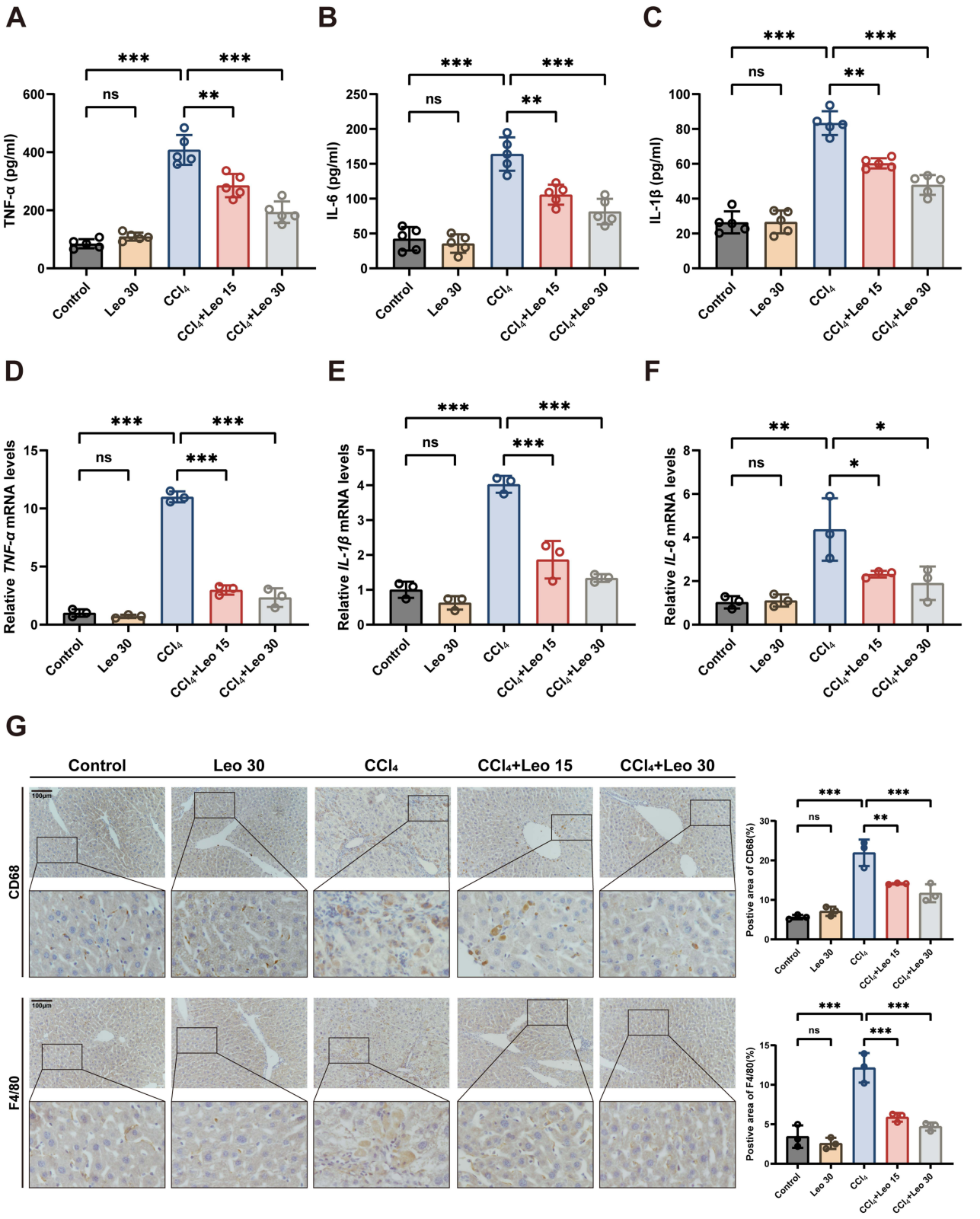

Figure 3 Leonurine inhibits the expression of inflammatory factors in the liver. (**A-C**) Serum inflammatory cytokines TNF-α (**A**), IL-6 (**B**) and IL-1β (**C**) were determined by ELISA. (**D-F**) The mRNA expression levels of TNF-α (**D**), IL-6 (**E**) and IL-1β (**F**) in mouse liver tissue by qRT-PCR. (**G**) Immunohistochemical images and quantitative analysis results of CD68 and F480 (scale bar, 100 μm). Data are expressed as mean ± standard deviation. *P<0.05, **P<0.01, ***P<0.001.
Abbreviation: ns, no significance.

https://doi.org/10.2147/DDDT.S518793

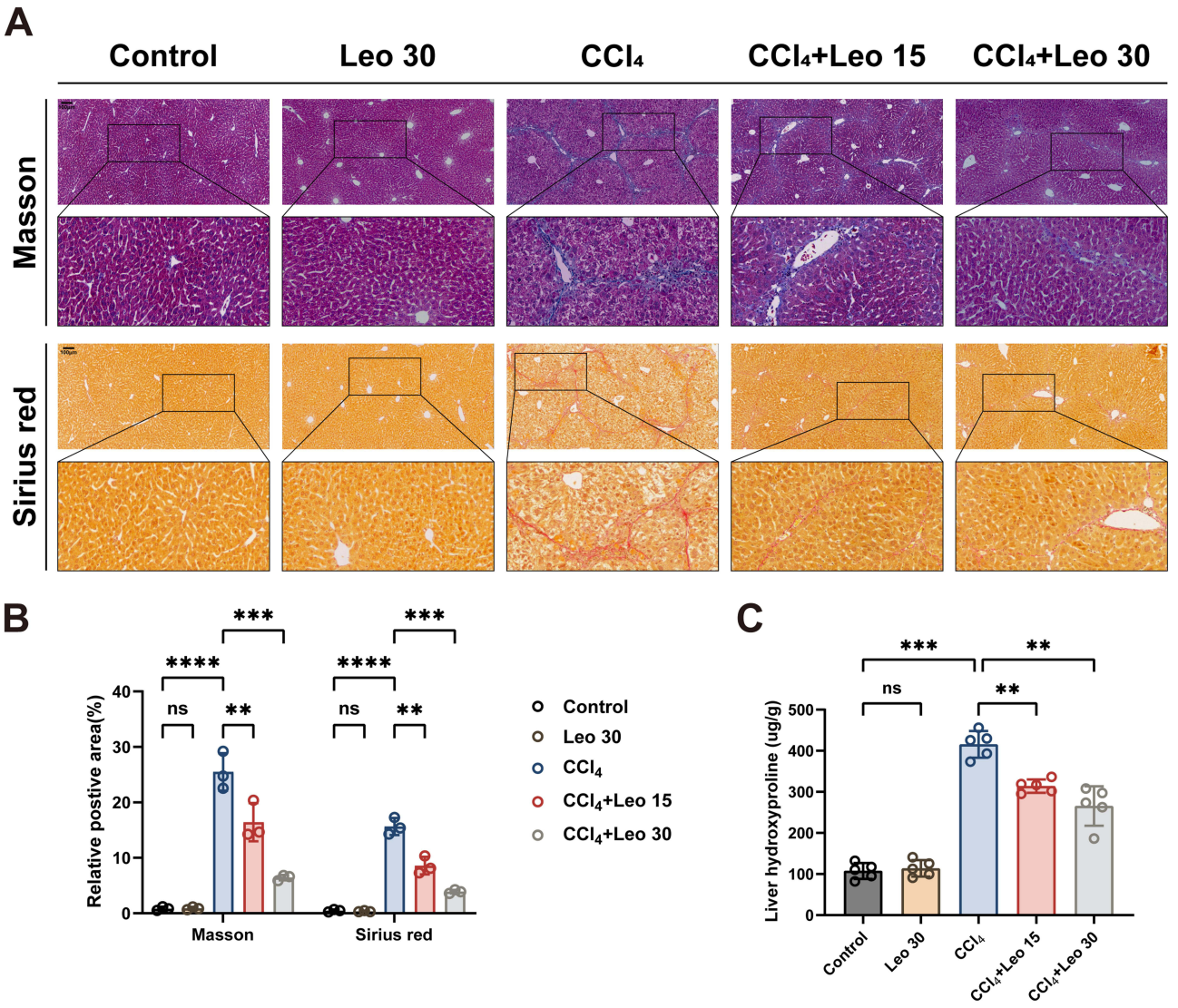

Figure 4 Leonurine alleviated CCl_4-induced liver fibrosis in mice. (**A-B**) Masson and Sirius red staining images (**A**) (scale bar, 100 μm) and quantitative analysis results (**B**). (**C**) Hydroxyproline in mouse liver tissue. Data are expressed as mean ± standard deviation. **P<0.01, ***P<0.001, ****P<0.0001.
Abbreviation: ns, no significance.

and PCNA. In contrast, there was no significant effect observed on the expression levels of CDK2 and CyclinE1. These findings indicate that Leo primarily inhibits the proliferation of LX-2 cells by interfering with the G1/S phase transition of the cell cycle (Figure 6C). Additionally, we examined the effect of Leo on the activation of HSCs in vitro, utilizing LX-2 cells as our model. As presented in Figure 6D, the control group exhibited the highest levels of α-SMA protein expression, indicative of complete activation of LX-2. However, treatment with Leo resulted in a downregulation of both α-SMA and COL1A1 protein levels. Moreover, qRT-PCR analysis was utilized to corroborate these findings at the mRNA level, confirming that the mRNA expressions of *α-SMA* and *COL1A1* in LX-2 cells decreased in response to increasing concentrations of Leo (Figure 6E). This trend aligns with the prior protein expression data. In summary, our findings strongly indicate that Leo inhibits HSC proliferation by disrupting cell cycle progression, thereby impeding HSC activation in vitro.

Leo Protects the Liver by Regulating Apoptosis

In the progression of liver fibrosis, apoptosis is acknowledged as a vital contributor to liver damage and healing. On one side, excessive apoptosis can lead to considerable loss of hepatocytes, which in turn affects both the liver's structure and function. On the other hand, the regulated apoptosis of HSCs may alleviate their activation and the transition towards fibrosis.[26] Western

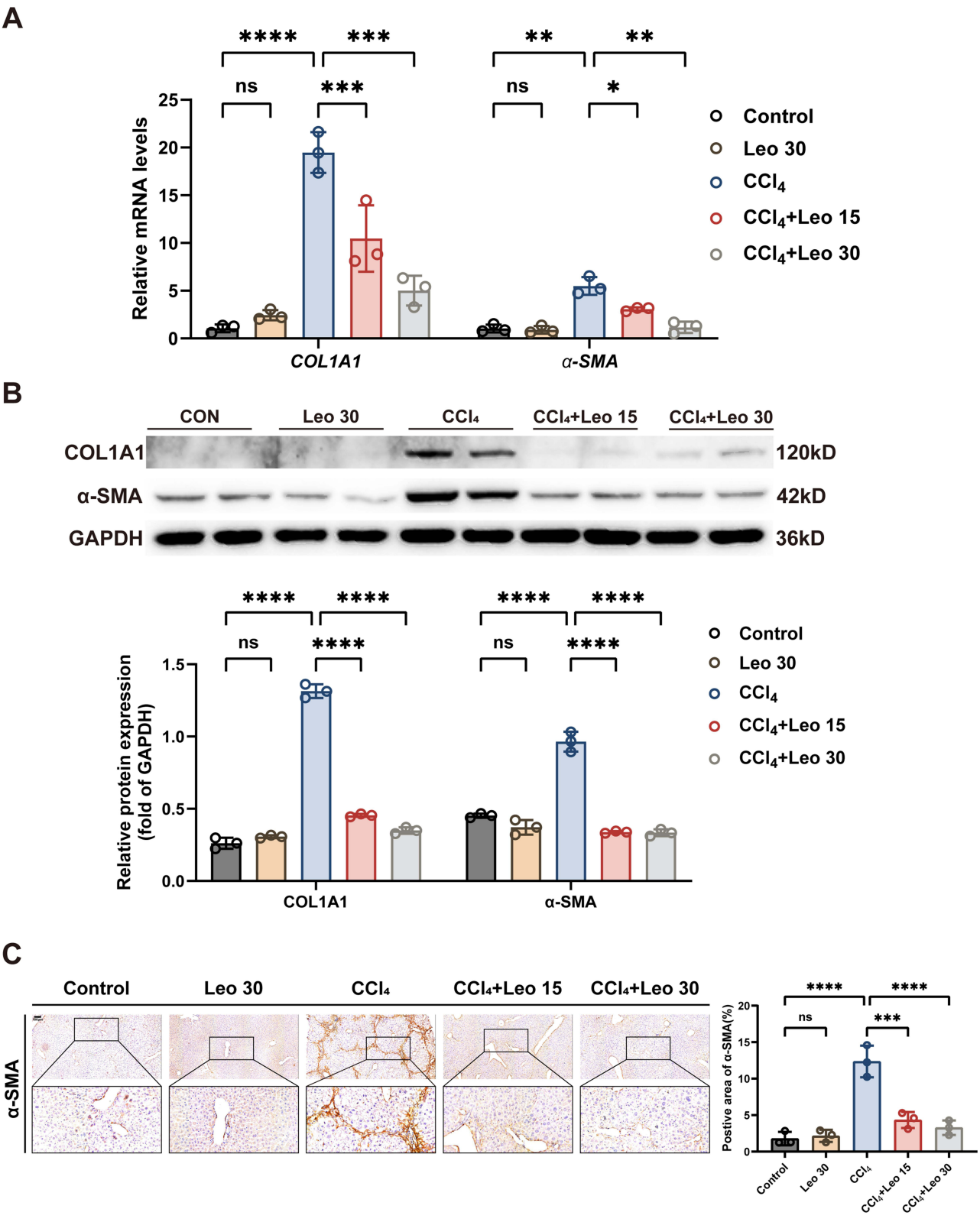

Figure 5 Leonurine inhibited HSC activation in vivo. (**A**) The mRNA expression levels of COL1A1 and α-SMA in mouse liver tissue by qRT-PCR. (**B**) The protein expression of COL1A1 and α-SMA in mouse liver tissue by Western blotting and quantitative analysis results. (**C**) Immunohistochemical images and quantitative analysis results of α-SMA (scale bar, 100 μm). Data are expressed as mean ± standard deviation. *P<0.05, **P<0.01, ***P<0.001, ****P<0.0001.
Abbreviation: ns, no significance.

https://doi.org/10.2147/DDDT.S518793

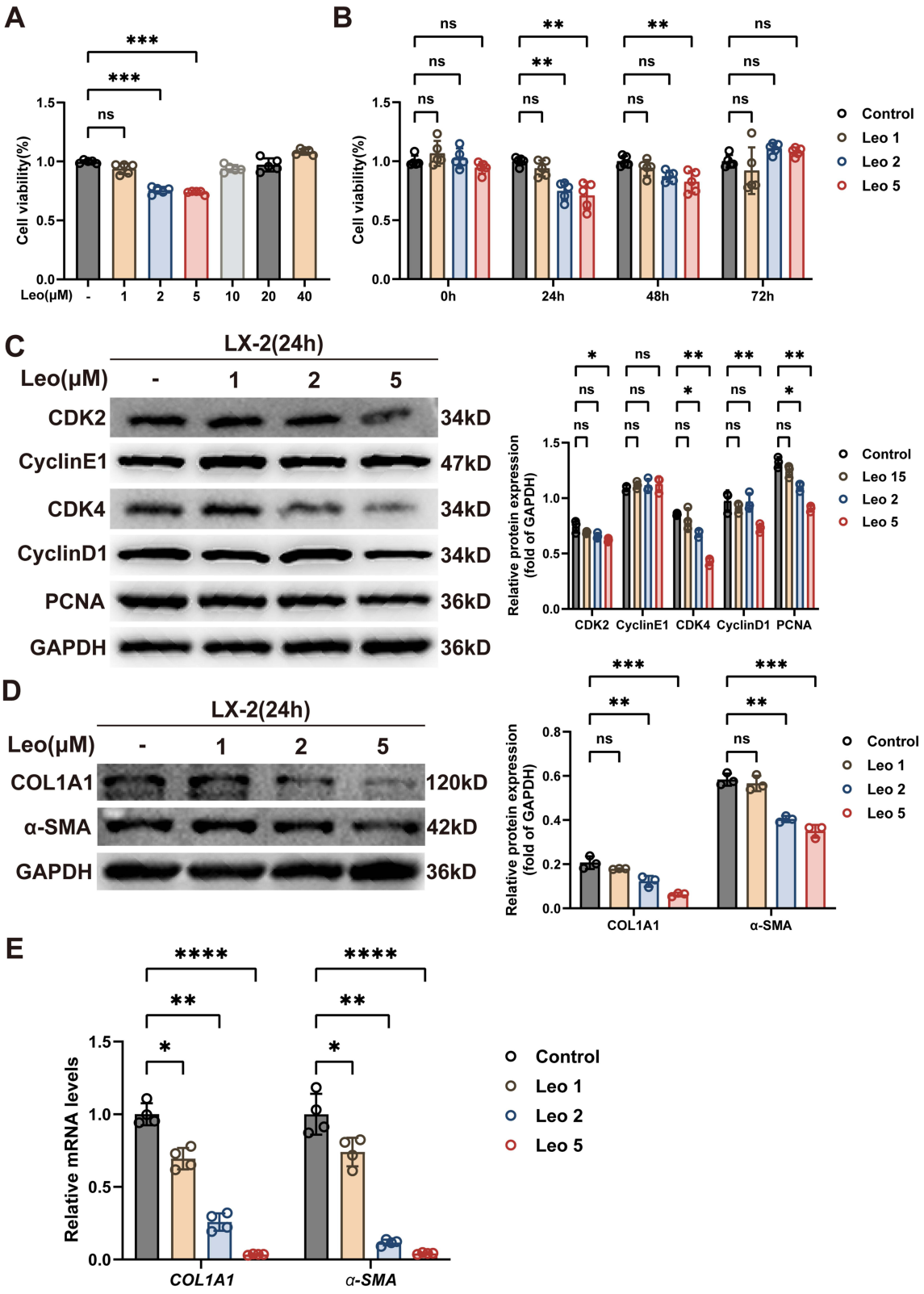

Figure 6 Leonurine inhibits HSC activation in vitro by delaying cell proliferation. (**A**) LX-2 cells were pretreated with Leo (1, 2, 5, 10, 20 or 40 μM), and cell viability was measured by CCK-8 assay. (**B**) LX-2 cells were pretreated with Leo (1, 2 or 5 μM) for 24, 48, or 72 h, and cell viability was measured by CCK-8 assay. (**C-D**) The protein expression of CDK2, CyclinE1, CDK4, CyclinD1 and PCNA (**C**) and COL1A1 and α-SMA (**D**) of LX-2 by Western blotting and quantitative analysis results. (**E**) The mRNA expression levels of COL1A1 and α-SMA of LX-2 by qRT-PCR. Data are expressed as mean ± standard deviation. *P<0.05, **P<0.01, ***P<0.001, ****P<0.0001.
Abbreviation: ns, no significance.

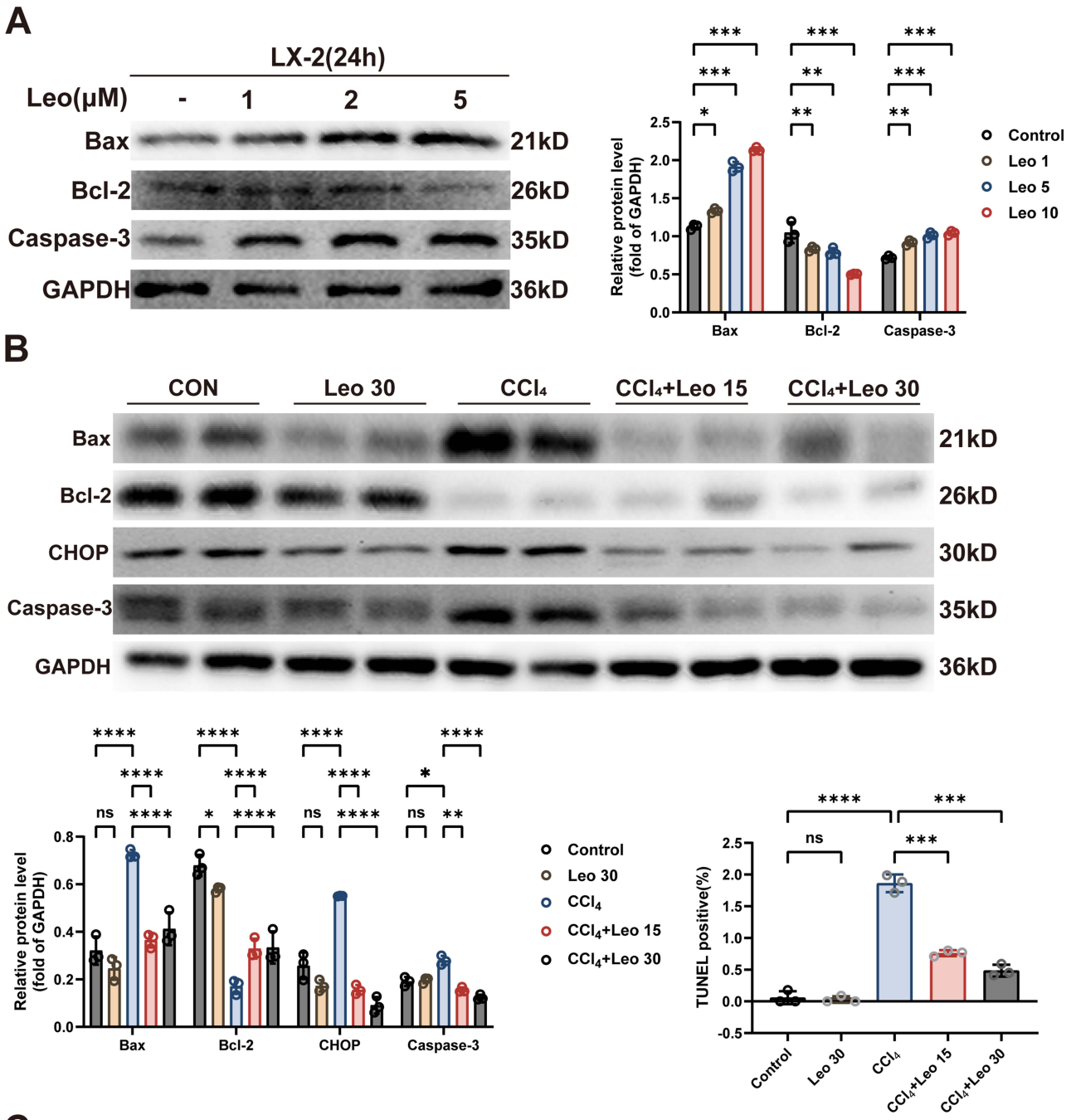

Figure 7 Leonurine protects the liver by regulating apoptosis. (**A**) The protein expression of Bax, Bcl-2, Caspase-3 of LX-2 by Western blotting and quantitative analysis results. (**B**) The protein expression of Bax, Bcl-2, CHOP and Caspase-3 in mouse liver tissue by Western blotting and quantitative analysis results. (**C**) TUNEL staining and quantification analysis (scale bar, 100 μm). Data are expressed as mean ± standard deviation. *P<0.05, **P<0.01, ***P<0.001, ****P<0.0001.
Abbreviation: ns, no significance.

https://doi.org/10.2147/DDDT.S518793

blot analysis was conducted to assess the expression levels of proteins associated with apoptosis. The findings revealed that treatment with Leo significantly elevated the levels of pro-apoptotic proteins, such as Bax and Caspase-3, in a dose-dependent manner. In contrast, the anti-apoptotic protein Bcl-2 exhibited a marked decrease under the same treatment conditions (Figure 7A). Subsequently, we investigated the impact of Leo on apoptosis within a mouse model of liver fibrosis that was induced by carbon tetrachloride (CCl_4). The animals in the CCl_4 group demonstrated a considerably higher expression of Bax, CHOP, and Caspase-3 when compared to the control group. Notably, treatment with Leo diminished the levels of these pro-apoptotic proteins in the context of CCl_4 exposure. Conversely, the expression of Bcl-2 exhibited an increase following Leo treatment, indicating a protective effect against apoptosis (Figure 7B). To delve deeper into Leo's effects on apoptosis in a living organism, we performed TUNEL staining to detect apoptosis in hepatocytes. The results, depicted in Figure 7C, indicated a significantly greater number of TUNEL-positive cells marked by green fluorescence in the CCl_4 group compared to the control group. Importantly, treatment with Leo led to a substantial reduction in hepatocyte apoptosis induced by CCl_4. These observations collectively suggest that Leo confers a protective effect against CCl_4-induced hepatocyte apoptosis in vivo, while simultaneously promoting apoptosis in hepatic stellate cells in vitro.

Leo Suppresses Liver Fibrosis Through the Modulation of the Hippo Pathway

The transcription factor YAP serves as a crucial downstream protein within the Hippo signaling pathway, affecting essential biological processes including cell growth, apoptosis, invasion, and migration. Recent research indicates a strong association between YAP activation in the liver and the progression of liver fibrosis. Importantly, levels of YAP expression are markedly heightened in liver tissues that are impacted by fibrosis. Overactivation of YAP results in enhanced cell proliferation and increased collagen deposition, which plays a role in the progression of liver fibrosis.[11,27] The initial assessment of the impact of Leo on YAP was conducted using Western blot analysis. The findings indicated that treatment with CCl_4 led to an increase in YAP protein levels when compared to the control group. In contrasting results, it was evident that Leo treatment significantly lowered the expression of YAP protein relative to the CCl_4 group (Figure 8A). This reduction was further corroborated through immunohistochemical analysis, which demonstrated a marked decrease in the number of YAP-positive cells following Leo treatment as opposed to the CCl_4 group (Figure 8B). This collective evidence strongly suggests that Leo may play a role in inhibiting the expression of YAP protein. Further investigations were carried out to explore the influence of Leo on the mRNA levels of *YAP*. Employing qRT-PCR techniques, the results presented indicated that Leo treatment led to a decline in the mRNA levels of *YAP* as well as its downstream targets, *ANKRD1* and *CTGF*, within LX-2 cells, especially in comparison to the control group (Figure 8C). Subsequently, the expression levels of proteins associated with the Hippo-YAP signaling pathway in LX-2 cells that had been pretreated with Leo were examined. The outcomes revealed an increase in the expression of p-LATS1/2 (Ser 909/872) and p-MST1/2 (Thr 183/180), both of which serve as negative regulators of YAP. Moreover, there was a notable downregulation of YAP expression alongside a significant increase in p-YAP (Ser 397) (Figure 8D). Previous research has indicated that YAP can undergo phosphorylation at various sites; in particular, phosphorylation at Ser 127 promotes YAP translocation to the cytoplasm, whereas phosphorylation at Ser 397 is linked to YAP protein degradation.[28,29] To gain further understanding of the role of YAP in the inhibition of HSCs activation by Leo, SiYAP was utilized to decrease YAP levels in LX-2 cells. The results obtained through Western blot analysis indicated that both the pretreatment with Leo and the transfection with SiYAP resulted in a reduction of YAP and α-SMA levels in comparison to the control group. Notably, the application of Leo did not lead to any additional decrease in α-SMA expression following the knockdown of YAP, as illustrated in Figure 8E. Furthermore, the subcellular localization of YAP was evaluated using IF. The findings revealed that in untreated LX-2 cells, YAP predominantly localized to the nuclei, as evidenced by the presence of green fluorescence. However, after treatment with Leo or the knockdown of YAP, there was a marked reduction in the levels of YAP expression. Importantly, there was no significant alteration in YAP expression when YAP knockdown was performed alongside Leo treatment (Figure 8F). These observations suggest that Leo may inhibit HSCs activation by acting on the Hippo/YAP signaling pathway.

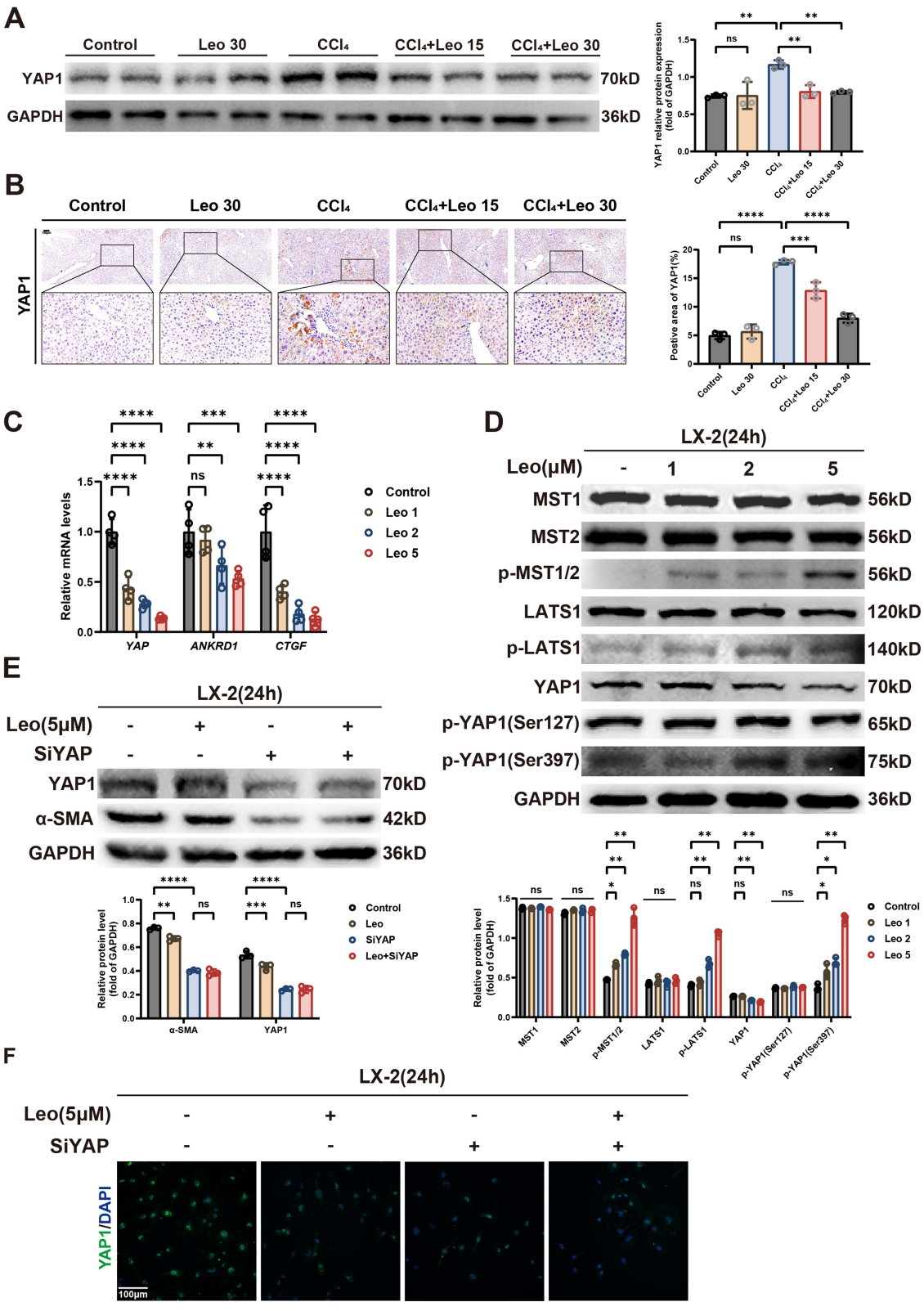

Figure 8 Leonurine inhibiting HSC activation by blocking Hippo-YAP signaling pathway. (**A**) The protein expression of YAP1 in mouse liver tissue by Western blotting and quantitative analysis results. (**B**) Immunohistochemical images and quantitative analysis results of YAP1 (scale bar, 100 μm). (**C**) The mRNA expression levels of YAP1, ANKRD1 and CTGF of LX-2 by qRT-PCR. (**D**) The protein expression of Hippo-YAP signaling pathway proteins of LX-2 by Western blotting and quantitative analysis results. (**E**) The protein expression of COL1A1 and α-SMA of LX-2 treated with Leo (5μM) and YAP SiRNA by Western blotting and quantitative analysis results. (**F**) Immunofluorescence staining for YAP1 (green) of LX-2 treated with Leo (5μM) and YAP SiRNA (scale bar, 100 μm). Data are expressed as mean ± standard deviation. *P<0.05, **P<0.01, ***P<0.001, ****P<0.0001.
Abbreviation: ns, no significance.

https://doi.org/10.2147/DDDT.S518793

Discussion

Our study demonstrates that leonurine (Leo) holds significant therapeutic potential for the treatment of liver fibrosis. Through the use of CCl_4-induced mouse models and LX-2 cell lines, we observed that Leo accelerates the recovery from liver damage and promotes fibrosis resolution. Specifically, Leo was found to suppress the proliferation of hepatic stellate cells (HSCs) and induce their apoptosis. Furthermore, Leo significantly reduced the expression of YAP by inhibiting the Hippo-YAP signaling pathway, thereby hindering the activation of HSCs and the progression of liver fibrosis. The evidence supporting Leo's anti-fibrotic effects is multifaceted: (i) in vivo, Leo enhanced the recovery from CCl_4-induced liver damage and fibrosis in mice; (ii) in vitro, Leo markedly arrested the cell cycle of HSCs, leading to reduced cellular proliferation; (iii) Leo decreased hepatocyte apoptosis in vivo while promoting HSC apoptosis in vitro; and (iv) Leo's inhibition of the Hippo-YAP signaling pathway resulted in decreased YAP expression, which is critical for preventing HSC activation and liver fibrosis advancement. These findings collectively underscore Leo's potential as a novel therapeutic agent for liver fibrosis.

HSC activation is pivotal for liver fibrosis progression, triggering substantial collagen production and accelerating hepatic fibrosis. Research indicates that Leo can modulate cyclin kinases, impact cell cycle stages, and regulate apoptosis signaling pathways.[16,30,31] Thus, targeting HSC cycle activity and apoptosis via Leo may offer a promising fibrosis treatment strategy. In our study, Leo (1, 2, 5 μM) significantly reduced LX-2 cell proliferation, with the most pronounced effect 24 hours post-treatment. Leo decreased levels of cell cycle proteins (CDK4 and CyclinD1) and the proliferation marker PCNA, suggesting G1/S phase arrest in HSCs.[32] Additionally, Leo reduces CCl_4-induced hepatocyte apoptosis in vivo while promoting HSC apoptosis in vitro. This dual effect not only alleviates liver damage but also inhibits HSC activation, a key mechanism in mitigating liver fibrosis. This is a crucial advancement in understanding how Leo impacts cellular processes related to liver health.[33]

Recent findings highlight a significant relationship between the Hippo-YAP pathway and the activation of HSCs.[11,34,35] Once activated by HSCs or myofibroblasts, YAP enters a prolonged activated state. It then translocates to the nucleus, upregulating target genes associated with liver fibrosis progression, such as ANKRD1 and CTGF.[10] This leads to further HSC activation, increased extracellular matrix (ECM) production, and worsened fibrosis.[10] The current findings suggest that Leo pretreatment results in the down-regulation of YAP expression in fully self-activated LX-2 cells. LX-2 cells, which are partially activated HSCs during in vitro culture, were utilized in this study. These cells exhibit self-activation characteristics due to their inherent properties and culture conditions. The self-activation of LX-2 cells is attributed to their spontaneous

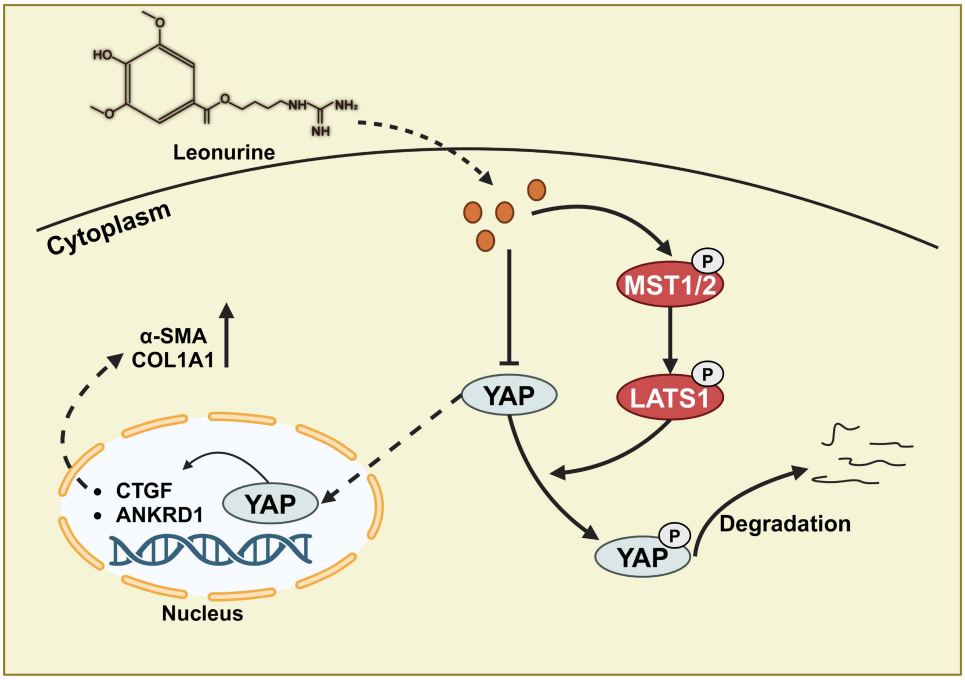

Figure 9 Schematic representation of Leonurine delaying the progression of liver fibrosis by blocking the Hippo-YAP pathway.

immortalization and response to growth factors like PDGF-BB and TGF-β1, which are prominent stimuli for HSC activation. This allows LX-2 cells to maintain a partially activated phenotype without undergoing any special procedures to promote activation. This aligns with certain methodologies described in earlier studies.[25,36,37] Furthermore, the treatment with Leo not only led to a marked reduction in YAP expression within liver tissues impacted by CCl_4-induced fibrosis but also modulated the MST-LATS kinase cascade, promoting the phosphorylation of YAP (Ser397). This process facilitates the degradation of YAP, consequently further reducing expression levels. The decreased expression of YAP results in a lower level of proteins essential to the fibrosis process, especially those regulated by YAP downstream. Importantly, YAP knockdown in LX-2 cells did not significantly lessen the inhibitory action of Leo on HSCs activation. These findings imply that Leo may alleviate liver fibrosis, likely through the modulation of the Hippo-YAP signaling pathway.

Conclusion

The findings of this research indicate that Leo has the capability to suppress the activation of HSCs in both in vivo and in vitro environments. This is significant as HSCs play a critical role in the development of liver fibrosis. Additionally, the research demonstrates that Leo effectively reduces the expression of target genes that are linked to hepatic fibrosis. This reduction is facilitated by the degradation of YAP proteins through the MST-LATS kinase signaling pathway once Leo penetrates the cells. The study provides a comprehensive understanding of the anti-fibrotic properties of Leo, as well as its specific mechanism for inhibiting the activation of HSCs (Figure 9). However, our study also has some limitations. The therapeutic effects of Leo were only evaluated in preclinical models, and its efficacy and safety in humans remain to be determined. Future research should focus on validating these findings in clinical trials and exploring the appropriate dosage and duration of Leo supplementation. Additionally, further studies are needed to investigate potential drug interactions, to ensure the safe and effective translation of Leo into clinical practice.

Data Sharing Statement

Data supporting the results in this study are available upon request from the corresponding authors.

Acknowledgments

This research received funding from various sources, including the National Natural Science Foundation of China (No. 82100647 and 82170587), Sichuan Science and Technology Program (NO. 2025ZNSFSC1685), Luzhou Science and Technology Program (NO. 2024JYJ048), and the Scientific Research Foundation of Southwest Medical University of China (NO. 2022QN029).

Disclosure

The authors declare that they have no conflicts of interest in this work.

References

1. Hammerich L, Tacke F. Hepatic inflammatory responses in liver fibrosis. *Nat Rev Gastroenterol Hepatol*. 2023;20(10):633–646. doi:10.1038/s41575-023-00807-x
2. Bai J, Qian B, Cai T, et al. Aloin attenuates oxidative stress, inflammation, and CCl 4 -induced liver fibrosis in mice: possible role of TGF-β/smad signaling. *J Agric Food Chem*. 2023;71(49):19475–19487. doi:10.1021/acs.jafc.3c01721
3. Parola M, Pinzani M. Liver fibrosis: pathophysiology, pathogenetic targets and clinical issues. *Mol Aspects Med*. 2019;65:37–55. doi:10.1016/j.mam.2018.09.002
4. Rockey DC, Friedman SL. Fibrosis regression after eradication of hepatitis C virus: from bench to bedside. *Gastroenterology*. 2021;160(5):1502–1520.e1. doi:10.1053/j.gastro.2020.09.065
5. Wang F-D, Zhou J, Chen E-Q. Molecular mechanisms and potential new therapeutic drugs for liver fibrosis. *Front Pharmacol*. 2022;13:787748. doi:10.3389/fphar.2022.787748
6. Zhang X, Sharma P, Maschmeyer P, et al. GARP on hepatic stellate cells is essential for the development of liver fibrosis. *J Hepatol*. 2023;79(5):1214–1225. doi:10.1016/j.jhep.2023.05.043
7. Breitkopf-Heinlein K, Martinez-Chantar ML. Targeting hepatic stellate cells to combat liver fibrosis: where do we stand? *Gut*. 2024;73(9):1411–1413. doi:10.1136/gutjnl-2023-331785
8. Meng Z, Moroishi T, Guan KL. Mechanisms of Hippo pathway regulation. *Genes Dev*. 2016;30(1):1–17. doi:10.1101/gad.274027.115
9. Zhao B, Li L, Tumaneng K, et al. A coordinated phosphorylation by Lats and CK1 regulates YAP stability through SCF β-TRCP. *Genes Dev*. 2010;24(1):72–85. doi:10.1101/gad.1843810

10. Xiang D. et al. Physalin D attenuates hepatic stellate cell activation and liver fibrosis by blocking TGF-β/Smad and YAP signaling. *Phytomedicine*, 2020. 78: p. 153294.
11. Du K, Maeso-Díaz R, Oh SH, et al. Targeting YAP-mediated HSC death susceptibility and senescence for treatment of liver fibrosis. *Hepatology*. 2023;77(6):1998–2015. doi:10.1097/HEP.0000000000000326
12. Wang P, Li J, Ji M, et al. Vitamin D receptor attenuates carbon tetrachloride-induced liver fibrosis via downregulation of YAP. *J Hazard Mater*. 2024;478:135480. doi:10.1016/j.jhazmat.2024.135480
13. Cao Q, Wang Q, Wu X, et al. A literature review: mechanisms of antitumor pharmacological action of leonurine alkaloid. *Front Pharmacol*. 2023;14:1272546. doi:10.3389/fphar.2023.1272546
14. Rong W, Li J, Pan D, et al. Cardioprotective mechanism of leonurine against myocardial ischemia through a liver-cardiac crosstalk metabolomics study. *Biomolecules*. 2022;12(10):1512. doi:10.3390/biom12101512
15. Shen S, Wu G, Luo W, et al. Leonurine attenuates angiotensin II-induced cardiac injury and dysfunction via inhibiting MAPK and NF-κB pathway. *Phytomedicine*. 2023;108:154519. doi:10.1016/j.phymed.2022.154519
16. Yu Y, Zhou S, Wang Y, et al. Leonurine alleviates Acetaminophen-induced acute liver injury by regulating the PI3K/AKT signaling pathway in mice. *Int Immunopharmacol*. 2023;120:110375. doi:10.1016/j.intimp.2023.110375
17. Zhang L, Li H-X, Pan W-S, et al. Novel hepatoprotective role of Leonurine hydrochloride against experimental non-alcoholic steatohepatitis mediated via AMPK/SREBP1 signaling pathway. *Biomed Pharmacother*. 2019;110:571–581. doi:10.1016/j.biopha.2018.12.003
18. Li Z, Chen K, Zhu YZ. Leonurine inhibits cardiomyocyte pyroptosis to attenuate cardiac fibrosis via the TGF-β/Smad2 signalling pathway. *PLoS One*. 2022;17(11):e0275258. doi:10.1371/journal.pone.0275258
19. Cheng H, Bo Y, Shen W, et al. Leonurine ameliorates kidney fibrosis via suppressing TGF-β and NF-κB signaling pathway in UUO mice. *Int Immunopharmacol*. 2015;25(2):406–415. doi:10.1016/j.intimp.2015.02.023
20. Liu XH, Pan -L-L, Deng H-Y, et al. Leonurine (SCM-198) attenuates myocardial fibrotic response via inhibition of NADPH oxidase 4. *Free Radic Biol Med*. 2013;54:93–104. doi:10.1016/j.freeradbiomed.2012.10.555
21. Xi T, Wang R, Pi D, et al. The p53/miR-29a-3p axis mediates the antifibrotic effect of leonurine on angiotensin II-stimulated rat cardiac fibroblasts. *Exp Cell Res*. 2023;426(1):113556. doi:10.1016/j.yexcr.2023.113556
22. Lei XF, Fu W, Kim-Kaneyama J-R, et al. Hic-5 deficiency attenuates the activation of hepatic stellate cells and liver fibrosis through upregulation of Smad7 in mice. *J Hepatol*. 2016;64(1):110–117. doi:10.1016/j.jhep.2015.08.026
23. Xu H, Hong S, Yan Z, et al. RAP-8 ameliorates liver fibrosis by modulating cell cycle and oxidative stress. *Life Sci*. 2019;229:200–209. doi:10.1016/j.lfs.2019.04.037
24. Dewidar B, Meyer C, Dooley S, et al. TGF-β in hepatic stellate cell activation and liver fibrogenesis-updated 2019. *Cells*. 2019;8(11):1419. doi:10.3390/cells8111419
25. Xiu AY, Ding Q, Li Z, et al. Doxazosin attenuates liver fibrosis by inhibiting autophagy in hepatic stellate cells via activation of the PI3K/Akt/mTOR signaling pathway. *Drug Des Devel Ther*. 2021;15:3643–3659. doi:10.2147/DDDT.S317701
26. Lu JL, Yu CX, Song LJ. Programmed cell death in hepatic fibrosis: current and perspectives. *Cell Death Discov*. 2023;9(1):449. doi:10.1038/s41420-023-01749-8
27. Dai Y, Hao P, Sun Z, et al. Liver knockout YAP gene improved insulin resistance-induced hepatic fibrosis. *J Endocrinol*. 2021;249(2):149–161. doi:10.1530/JOE-20-0561
28. Zhao W, Liu H, Wang J, et al. Cyclizing-berberine A35 induces G2/M arrest and apoptosis by activating YAP phosphorylation (Ser127). *J Exp Clin Cancer Res*. 2018;37(1):98. doi:10.1186/s13046-018-0759-6
29. Tu K, Yang W, Li C, et al. Fbxw7 is an independent prognostic marker and induces apoptosis and growth arrest by regulating YAP abundance in hepatocellular carcinoma. *Mol Cancer*. 2014;13(1):110. doi:10.1186/1476-4598-13-110
30. Lin M, Pan C, Xu W, et al. Leonurine promotes cisplatin sensitivity in human cervical cancer cells through increasing apoptosis and inhibiting drug-resistant proteins. *Drug Des Devel Ther*. 2020;14:1885–1895. doi:10.2147/DDDT.S252112
31. Liang F, Xu X, Tu Y. Resveratrol inhibited hepatocyte apoptosis and alleviated liver fibrosis through miR-190a-5p /HGF axis. *Bioorg Med Chem*. 2022;57:116593. doi:10.1016/j.bmc.2021.116593
32. Baker SJ, Poulikakos PI, Irie HY, et al. CDK4: a master regulator of the cell cycle and its role in cancer. *Genes Cancer*. 2022;13:21–45. doi:10.18632/genesandcancer.221
33. Xu L, Gu L, Tao X, et al. Effect of dioscin on promoting liver regeneration via activating Notch1/Jagged1 signal pathway. *Phytomedicine*. 2018;38:107–117. doi:10.1016/j.phymed.2017.11.006
34. Li C, Zhang R, Zhan Y, et al. Resveratrol inhibits hepatic stellate cell activation via the hippo pathway. *Mediators Inflamm*. 2021;2021:3399357. doi:10.1155/2021/3399357
35. Salloum S, Jeyarajan AJ, Kruger AJ, et al. Fatty acids activate the transcriptional coactivator YAP1 to promote liver fibrosis via p38 mitogen-activated protein kinase. *Cell Mol Gastroenterol Hepatol*. 2021;12(4):1297–1310. doi:10.1016/j.jcmgh.2021.06.003
36. Meng D, Li Z, Wang G, et al. Carvedilol attenuates liver fibrosis by suppressing autophagy and promoting apoptosis in hepatic stellate cells. *Biomed Pharmacother*. 2018;108:1617–1627. doi:10.1016/j.biopha.2018.10.005
37. Zhang Z, Guo M, Li Y, et al. RNA-binding protein ZFP36/TTP protects against ferroptosis by regulating autophagy signaling pathway in hepatic stellate cells. *Autophagy*. 2020;16(8):1482–1505. doi:10.1080/15548627.2019.1687985